DOI: 10.1021/ma900266s

Macromolecules
ARTICLE

Complex Thermal and Bulk Assembling Properties of Dendritic−Linear−Dendritic Triblock Copolymers Depending on the Length of the Middle Block

Eunji Lee,[‡] Byung-Ill Lee,[†] Seung-Hyun Kim,[†] Jeong-Kyu Lee,[§] Wang-Cheol Zin,[§] and Byoung-Ki Cho*,[†]

[†]*Department of Chemistry and Center for Photofunctional Energy Materials (CPEM), Dankook University, Gyeonggi-Do, 448-701, Korea,* [‡]*Department of Chemistry, Yonsei University, Shinchon 134, Seoul 120-749, Korea, and* [§]*Department of Materials Science and Engineering, Pohang University of Science and Technology, Pohang 790-784, Korea*

Received February 5, 2009; Revised Manuscript Received May 11, 2009

ABSTRACT: We report the synthesis, as well as the complex thermal and assembling properties, of a series of three triblock copolymers **1**−**3**, each of which is based on aliphatic polyether third-generation dendron ends that contain tetradecyl peripheries and a hydrophilic linear poly(ethylene oxide) (PEO) middle block. Because of the large cross section of the third-generation dendron ends and the amorphous PEO-like dendritic core, the crystallinity of the central PEO coil in each block copolymer is significantly reduced. In particular, copolymers **1** and **2** with relatively short PEO coils (M_n = 1000 and 2000 g/mol) revealed no PEO melting. Also, the crystallinity of the peripheral tetradecyl chains was investigated, depending on the PEO morphology. Copolymers **1** and **2**, both with amorphous PEO coils, had similar degrees of the tetradecyl crystallinity, 33% and 34%, respectively, while copolymer **3**, with a crystalline PEO coil (M_n = 4000 g/mol), showed a somewhat higher value of 41%. This is probably due to the hard confinement effect caused by the crystalline PEOs during the tetradecyl crystallization of copolymer **3**. In addition to surveying the thermal behavior of the copolymers, their self-assembling behavior was surveyed in the crystalline and liquid crystalline (mesophase) states by SAXS and TEM techniques. The copolymers showed a complex bulk morphological behavior as a function of the PEO coil length. In the crystalline state, copolymers **1** and **2** exhibited columnar assemblies, but they showed different column packing (i.e., oblique and rectangular symmetries for **1** and **2**, respectively). Meanwhile, copolymer **3** formed lamellar structures in both of its crystalline states. In the molten states, all copolymers showed microphase-separated microstructures, as indicated by the SAXS and TEM results. Copolymer **1** exhibited a cylindrical mesophase without a long-range order, while copolymers **2** and **3** showed hexagonal columnar and disordered cylindrical mesophases as temperature increased.

Introduction

Variation in polymer chain architecture is a crucial parameter that dictates the self-assembly behavior of block copolymers. Advances in polymer synthesis now make it possible to investigate block copolymers that are more complex than easily accessible linear−linear block copolymers,[1] such as complicated block copolymers that share both dendritic and linear coil blocks.[2] In comparison with linear−linear block copolymers, dendritic−linear block copolymers are expected to show distinct self-assembly behaviors because of the greater chain asymmetry between the branched dendritic blocks and the unbranched linear blocks.[3] The self-assembly of dendritic−linear block copolymers has been investigated both in solution[4] and in the bulk states,[5] and the generation of dendritic blocks is highly dependent on microstructural morphology.

Among the reported self-assembling dendritic−linear block copolymers, block copolymers bearing hydrophobic crystalline alkyl chains on the dendron periphery and hydrophilic poly (ethylene oxide) (PEO) coils have exhibited well-defined assembling features in the bulk states.[6] The enhanced microphase segregation arises from the high incompatibility between the alkyl and the PEO blocks. Recently, we reported on a dendritic−linear block copolymer system that bears aliphatic polyether dendrons and a linear poly(ethylene oxide) coil and investigated its self-assembly behavior in the molten state.[7] In that study, we demonstrated that variation in the generaton of the dendron at a fixed linear coil leads to diverse liquid crystalline morphologies, including A15 micellar, hexagonal columnar, bicontinuous cubic, and lamellar mesophases. Furthermore, the temperature-dependent phase sequences are completely the reverse of those found in linear−linear block copolymers. Despite the interesting mesomorphic behavior, the microstructures in the crystalline states were shown to be solely lamellar structures, which have been found in other analogous dendritic−linear block copolymers.[6a−6c] With respect to the dendron peripheries, dendritic−linear block copolymers that have a solid-state lamellar organization usually contain long crystalline alkyl peripheries, such as octadecyl, docosyl, and stearate groups. Because of the elongated alkyl chain lengths, the melting transitions of the peripheries occur at higher temperatures than those of linear PEO blocks, and from the anisotropic organization of the long peripheries in the crystalline state, the lamellar assembly is believed to be favorable.

In this paper, we designed a series of three dendritic−linear−dendritic triblock copolymers (copolymers **1**−**3**), consisting of a

*To whom all correspondence should be addressed. E-mail: chobk@dankook.ac.kr.

 Published on Web 05/28/2009

Scheme 1. Synthesis of Triblock Copolymers 1−3

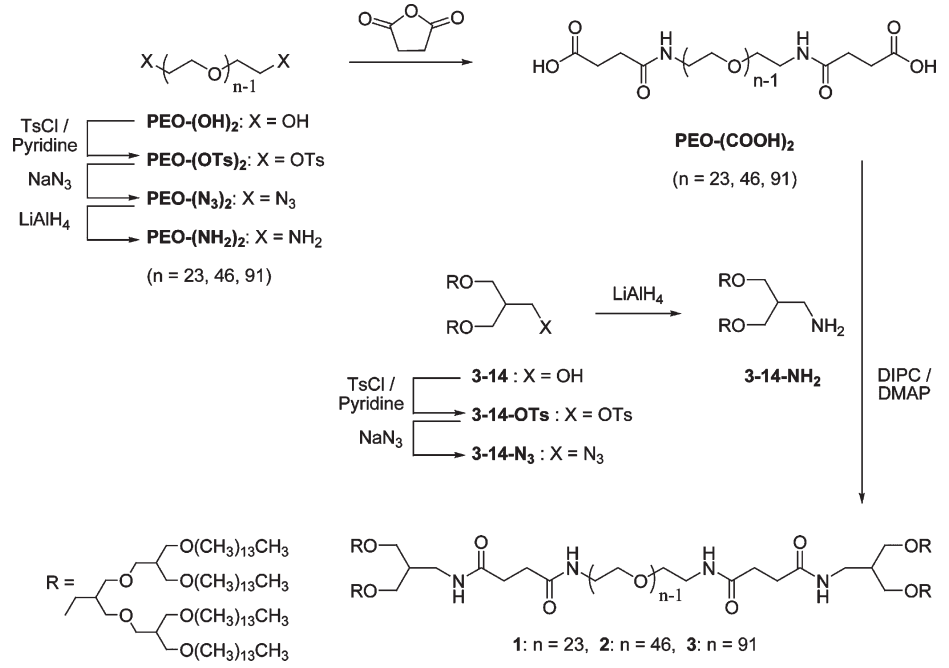

third-generation aliphatic polyether dendritic core and linear PEO coils of different lengths (Scheme 1). In comparison with the above-mentioned examples,[6a−6c] the main strategy in block copolymers is to minimize the length of the alkyl peripheries. In this work, we employed tetradecyl chains as peripheral groups that have fewer methylene units than do octadecyl and stearate groups. By such a molecular design, the triblock copolymers might have reduced molecular anisotropies that influence thermal (e.g., melting transition and crystallinity) and assembling properties in the bulk states. Particularly, despite the alkyl crystallization generally forcing a lamellar morphology, the short tetradecyl peripheries, we expected, cannot produce enough molecular anisotropy to form a lamellar organization. Therefore, complex nanostructures might be developed in the solid states as well as in the molten state. As a consequence of this work, we observed rich assembled nanostructures of oblique, rectangular, hexagonal, disordered columnar, and lamellar types, depending on the length and morphology (crystalline or amorphous) of the middle PEO block. In this paper, the details of the thermal and assembling properties of these copolymers are addressed.

Results and Discussion

Synthesis. The synthesis of the third-generation dendritic block, containing the aliphatic polyether dendritic core and tetradecyl peripheries, was reported previously.[8] As a middle linear block, we employed poly(ethylene oxide) (PEO) coils with number-average molecular weights of 1000, 2000, and 4000 g/mol for copolymers **1**−**3**, respectively. The hydroxyl ends of the dendron and of the PEO coils were converted into amine groups by the following reaction sequence: (i) tosylation by tosyl chloride, (ii) azidation by sodium azide, and (iii) reduction by lithium aluminum hydride. For the coupling of the dendron and linear coil segments, the PEO coil ends were functionalized with carboxylic acid groups by reacting with an excess of succinic anhydride. The final coupling reaction of the carboxylic acid-terminated PEOs (PEO-$(COOH)_2$) and the amine-terminated third-generation dendron (3-14-NH_2) was performed by using N,N′-diisopropylcarbodiimide (DIPC) in the presence of 4-(dimethylamino)pyridine (DMAP).

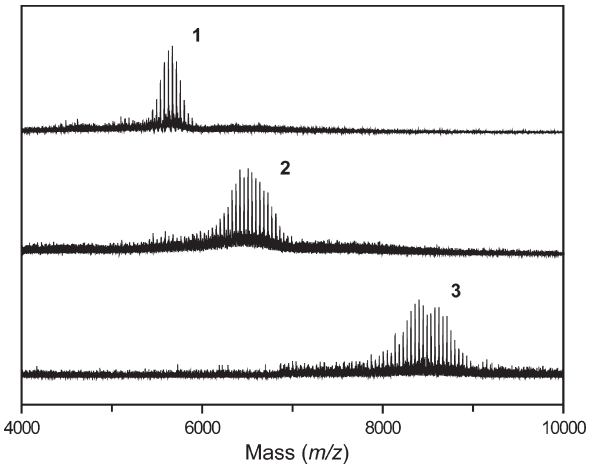

Figure 1. MALDI-TOF mass spectra of **1**−**3**.

The resulting triblock copolymers (**1**−**3**) were characterized by ^1H and ^{13}C NMR as well as by matrix-assisted laser desorption ionization time-of-flight mass spectrometry (MALDI-TOF MS), elemental analysis (EA), and gel permeation chromatography (GPC). All copolymers showed narrow polydispersities (M_w/M_n) of less than 1.06 in GPC and exhibited signals for the α-protons to the carbonyl groups near 2.49 ppm. Elemental analysis data of copolymers **1**−**3** were also in good agreement with the theoretical values.

Figure 1 shows the MALDI-TOF mass spectra of copolymers **1**−**3**. The M_n values were estimated to be 5614, 6443, and 8379 g/mol, respectively. These molecular weights are consistent with the theoretical M_n values to within a 3% error range. In addition, their polydispersities from MALDI-TOF MS are very close to one, which is indicative of high purity (Table 1).

Thermal Properties. The thermal behavior of copolymers **1**−**3** was studied by differential scanning calorimetry (DSC) and by temperature-dependent wide-angle X-ray scattering (WAXS) techniques. The results are summarized in Table 1.

Table 1. Characterization of Block Copolymers 1−3

copolymers	M_n (g/mol) MALDI-TOF MS	PDI (M_w/M_n)[a]	volume fraction of tetradecyl group (f_v)	phase transitions (°C) and corresponding enthalpy changes (J/g)[b]	crystallinity[c]	
					PEO	tetradecyl
1	5613.5	1.03	0.63	k 20.4 (53.2) dm 130 iso	none	0.33
2	6442.7	1.05	0.55	k 21.0 (47.3) hex 55 dm	none	0.34
3	8378.7	1.06	0.44	k 25.3 (44.4) k 39.9 (51.7) hex 105 dm	0.59	0.41

[a] From GPC. [b] Second heating data from DSC. [c] Crystallinity = experimental heat of fusion of a sigle PEO (tetradecyl group)/heat of fusion of a perfect crystalline PEO (tetradecyl group). Experimental heat of fusion of a PEO (tetradecyl group) (kJ/mol) = heat of fusion (J/g) from DSC × mass of a PEO (tetradecyl group)/weight fraction. The heat of fusion of a single perfect crystalline PEO (tetradecyl group) was calculated on the basis of the heat of fusion of a repeat unit in the perfect crystalline of 8.4 kJ/mol (4.11 kJ/mol). k = crystalline, dm = disordered mesophase, hex = hexagonal columnar, iso = isotropic liquid.

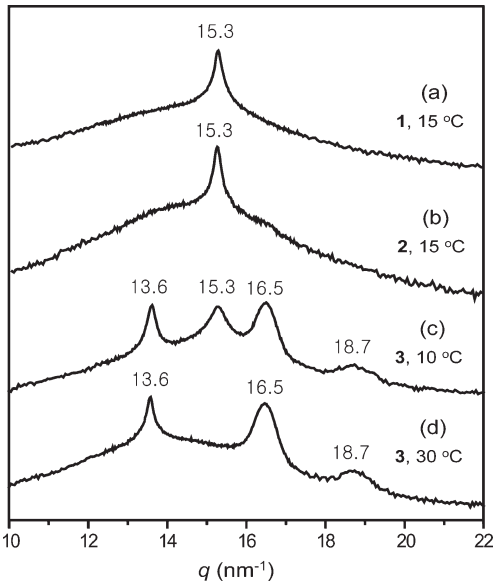

Figure 2. Wide-angle scattering patterns of triblock copolymers **1**−**3**.

DSC experiments were performed at a rate of 1.0 °C/min in the temperature range from −70.0 to 120.0 °C. The DSC data of copolymers **1** and **2** displayed first-order transitions at 20.4 and 21.0 °C, respectively, which correspond to the melting points of the tetradecyl peripheries. Surprisingly, no PEO melting transition was observed in copolymers **1** and **2**, although their homo-PEOs displayed their melting temperatures near 40.0 and 50.0 °C, respectively. Meanwhile, copolymer **3** showed two melting transitions, at 25.3 and 39.9 °C, for the tetradecyl and PEO parts, respectively. The assignment of the melting transitions can be confirmed by a temperature-variable WAXS technique. As shown in Figure 2a,b, the WAXS data of copolymers **1** and **2** detected at 15 °C revealed only one reflection at $q = 15.3\ nm^{-1}$, which is attributed to the crystal packing of the tetradecyl peripheries. On the other hand, the WAXS data of copolymer **3** at 10 °C displayed three additional reflections at $q = 13.6$, 16.5, and 18.7 nm^{-1}, together with the tetradecyl crystal peak at 15.3 nm^{-1} (Figure 2c). The additional reflections are a typical WAXS pattern of the monoclinic crystal structure of PEO.[9] When heated to 30 °C in the second crystalline state, the tetradecyl crystalline peak disappeared, and only the PEO crystal peaks remained (Figure 2d).

From the DSC and WAXS data, the relatively short PEO coils (M_n = 1000 and 2000 g/mol) of copolymers **1** and **2** did not crystallize, but instead they formed fully amorphous liquid states. This might be due to the large cross section of the third-generation dendron. As the cross-sectional area is larger, the attached linear coil inevitably adopts more folded, instead of extended, conformations. Because chain-folding regions are amorphous, more chain folding would result in a larger reduction of crystallinity. Particularly, the PEO coils in copolymers **1** and **2** have small molecular weights relative to copolymer **3**; thus, **1** and **2** easily become fully amorphous because, under the same generation dendron, the degree of chain folding would be the s ame regardless of the PEO's molecular weight. Of course, this effect is equally applied to copolymer **3**. From the DSC data, the PEO crystallinity of copolymer **3** was estimated to be 59%. This value is considerably smaller than the compositionally analogous polyalkane-*b*-poly (ethylene oxide) copolymers, where PEO crystallinities usually exceed 70%.[10] In addition to the dendron size effect, a plasticization effect of the amorphous hydrophilic dendritic core might influence the crystallinity to some extent.[2a] Since the basic repeating unit of aliphatic polyether dendritic cores (i.e., $CH_2CH(CH_2O)_2$) is almost identical to a doubled poly(ethylene oxide) structural unit, $2 \times (CH_2CH_2O)$, it is probable that the dendritic cores plasticize the crystalline linear PEO coils. Consequently, because of these factors, the PEO coils of copolymers **1** and **2** completely lost the crystallinity, and the PEO crystallinity of copolymer **3** was reduced.

Although the PEO crystallinities of all of the block copolymers were reduced or eliminated, copolymers **1** and **2** are fundamentally different from copolymer **3** in terms of PEO morphology. In other words, the PEO coils of copolymer **3** are still semicrystalline, while those of copolymers **1** and **2** are fully amorphous. Thus, we thought that the thermal properties of the tetradecyl peripheries might be distinctly influenced by the PEO morphology. In Table 1, the tetradecyl melting temperatures of copolymers **1** and **2** were shown to be 20.4 and 21.0 °C, respectively, which are nearly identical. However, the tetradecyl melting of **3** occurred at 25.3 °C. Furthermore, the degrees of crystallinity as obtained from the enthalpy changes for the melting transitions were calculated to be 33, 34, and 41% for **1**−**3**, respectively. Considering the DSC and WAXS data of copolymers **1** and **2**, the amorphous PEO coils do not confine the tetradecyl groups during the tetradecyl crystallization because the PEO coils are flexible. On the contrary, the precrystallized PEOs of copolymer **3** strongly confine the tetradecyl peripheries during the alkyl crystallization, which might have led to an enhanced crystal packing of the tetradecyl peripheries. Thus, it can be hypothesized that the hard confinement effect ($T_{m(PEO)} > T_{m(tetradecyl)}$) of the crystalline PEOs enhanced the tetradecyl crystallinity of copolymer **3**. It should be noted that the thermal behavior of copolymer **3** is considerably different from other double-crystalline PE-*b*-PEO copolymer systems, where PEO coils become molten before the melting of long alkyl chains; thus, the crystallization process of molten linear PEO coils was governed by the crystalline alkyl chains.[6a−6c,7,10b] The different thermal histories between this system and others are attributed to the length of the alkyl peripheries. Thus, by varying the alkyl chain length,

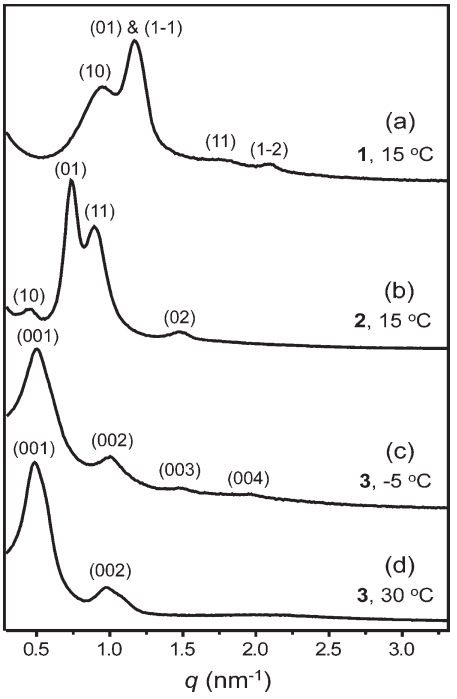

Figure 3. SAXS patterns of copolymer **1**−**3** in the crystalline states.

the thermal behavior of dendritic−coil block copolymer systems can be elaborately modulated.

Self-Assembly in the Crystalline Phases. In addition to their thermal behavior, the self-assembly of the triblock copolymers in their solid states was expected to be strongly influenced by the PEO morphology (i.e., crystalline or amorphous). To investigate the microstructures in the crystalline phases, SAXS experiments were performed. The SAXS data of copolymers **1** and **2** were detected at 15 °C at which, as was already characterized by the DSC and WAXS results, only the tetradecyl peripheries are crystalline. In Figure 3a, the SAXS data of copolymer **1** showed multiple reflections with q-spacing ratios of 1:1.23:1.83:2.21. Considering the q-spacing ratios, the nanostructure is not conventional lamellar nor is it a hexagonal columnar one. The analysis of the pattern was performed on the basis of the following equation:

$$\frac{q^2}{(2\pi)^2} = \frac{h^2}{(a\sin\gamma)^2} - \frac{2hk\cos\gamma}{ab\sin^2\gamma} + \frac{k^2}{(b\sin\gamma)^2}$$

where $q = 4\pi\sin\theta/\lambda$ (θ: the scattering angle; λ: the wavelength of X-ray beam), h and k are Miller indices of the scattering planes, a and b are unit-cell basis vectors, and γ is the angle between a and b ($0° < \gamma < 180°$).[11]

Using this equation, the SAXS reflections of copolymer **1** could be indexed as (10), (01), ($1\bar{1}$), (11), and ($1\bar{2}$), which agrees with a 2-D oblique lattice with lattice parameters a = 7.04 nm, b = 5.73 nm, and γ = 110.2°. To corroborate the microstructural details, transmission electron microscopy (TEM) experiments were conducted. The samples were microtomed to a thickness of ca. 50−70 nm and stained with RuO_4 vapor, which selectively stained the PEO.[12] As shown in Figure 4a, a bright-field TEM image of copolymer **1** at 15 °C revealed alternating light and dark regions. From the image, either a 2-D columnar or a 1-D lamellar morphology can be proposed. However, considering the 2-D oblique lattice from the SAXS data, the nanostructure can be assigned as a 2-D oblique columnar structure (Figure 5a). The column-to-column distance from the TEM image was

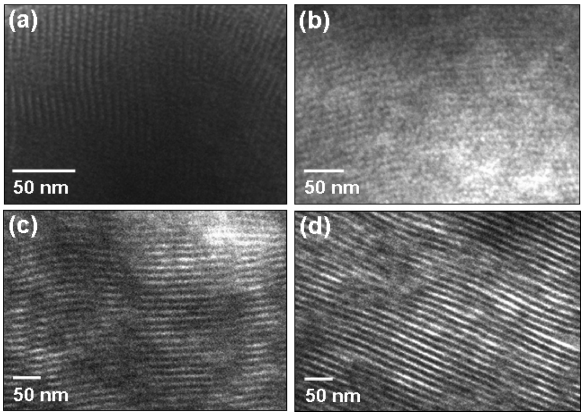

Figure 4. TEM images of ultramicrotomed films at (a) 15 °C for copolymer **1**, (b) 15 °C for copolymer **2**, and (c, d) −5 and 15 °C for copolymer **3**, respectively, stained with RuO_4.

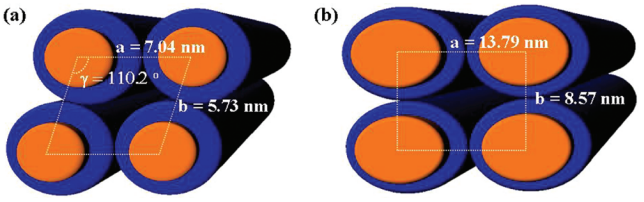

Figure 5. Schematic sketches of (a) the oblique columnar crystalline structure of copolymer **1** and (b) the rectangular columnar structure of copolymer **2**. The dark blue and orange colors indicate the crystalline alkyl peripheries and amorphous dendritic cores plus molten PEO coils, respectively.

estimated to be ~6.5 nm, which is close to the lattice parameters determined by the SAXS data.

Copolymer **2** exhibited a somewhat different SAXS pattern from copolymer **1** in the crystalline state at 15 °C. In Figure 3b, the SAXS pattern displayed four reflections with q-spacing ratios of 1:1.61:1.94:3.22. These reflections fit the reciprocal lattice planes of (10), (01), (11), and (02) of a rectangular columnar structure where γ is 90.0° (Figure 5b). The lattice parameters were calculated to be a = 13.79 nm and b = 8.57 nm. The TEM image of copolymer **2** at 15 °C also exhibited a columnar array (Figure 4b). In the image, the intercolumn distance is about 11.0 nm, which is approximately consistent with the SAXS lattice parameters.

It is interesting to note that the observed columnar morphologies of copolymers **1** and **2** are different from the commonly observed hexagonal columnar one. This is probably due to the fact that the cross sections of the constituent columns might not be circular but instead elliptical because cylinders with a circular cross section tend to form into a 2-D hexagonal symmetry. The driving force for the packing deviation from a hexagonal symmetry must be attributed to the crystallization of the tetradecyl peripheries that presumably results in the elliptical cross sections (Figure 5).[13] Of course, such rectangular or oblique columnar structures have been observed in only a few dendrimers and dendrons.[6d,14] In those cases, however, the driving forces for the nonsymmetrical columns were proposed as the anisotropic arrangements of mesogenic aromatic groups, and furthermore their supramolecular assemblies were modulated by changing either the number of peripheral groups or the generation number. In this sense, the column packing change from oblique to rectangular symmetries via the simple variation of the middle PEO length suggests an alternative way to fine-tune the solid-state supramolecular assemblies in dendritic building blocks. In addition, the

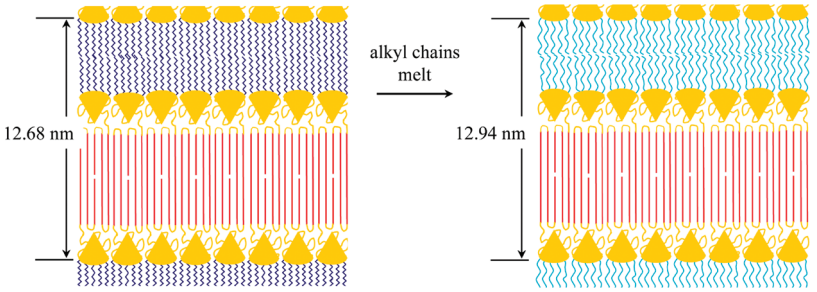

Figure 6. Sketches of the lamellar assemblies of copolymer **3** in the two crystalline states. Dark blue: crystalline alkyl chains; cyan: molten alkyl chains; red: crystalline PEOs; orange: molten PEOs and amorphous dendritic cores.

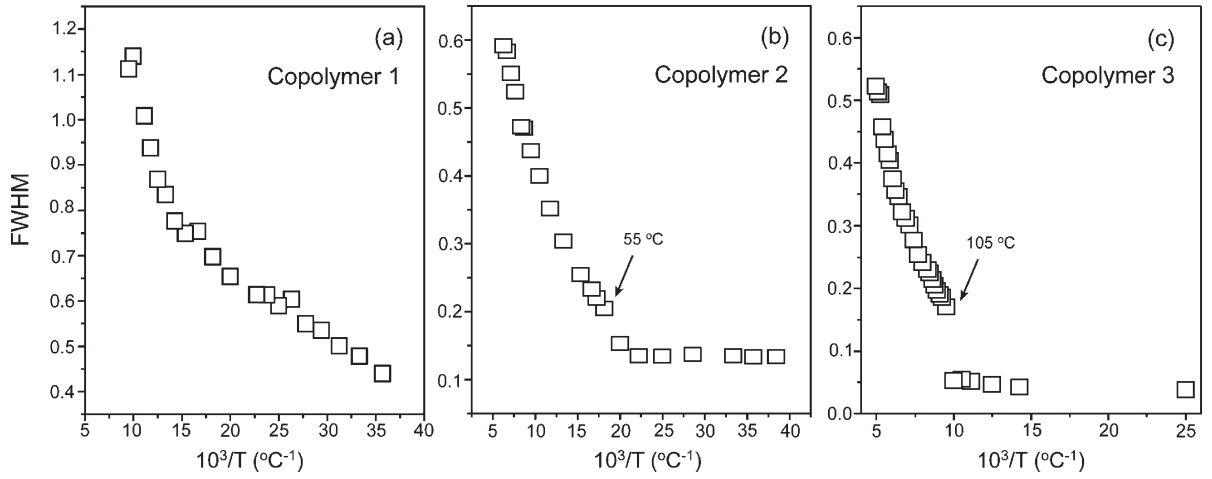

Figure 7. Plots of the full width at half-maximum (fwhm) of primary peak vs the reciprocal of the temperature.

assembly behavior of copolymers **1** and **2** is considerably different from lamellar assemblies seen in analogous dendritic−linear block copolymers that bear longer crystalline alkyl peripheries.[6a−6c,7] The assembling distinction can be elucidated by the less anisotropic overall molecular shape consisting of the short tetradecyl peripheries, thus favoring organization into columnar structures. On the contrary, other analogues contain longer alkyl peripheries, such as octadecyl, docosyl, and stearate chains. Therefore, the crystallization of longer alkyl chains would give rise to greater molecular anisotropy, thus favoring lamellar assembly.

In contrast to copolymers **1** and **2**, copolymer **3** showed two different crystalline phases as a function of temperature. Both crystalline states were investigated by SAXS experiments. Figure 3c is the SAXS pattern in the lower temperature crystalline phase, where both the PEO coil and the tetradecyl peripheries are crystalline. The pattern exhibited four reflections with q-spacing ratios of 1:2:3:4, which indicates a lamellar structure with a periodic layer thickness of 12.68 nm. Upon heating, in the second crystalline state, where the tetradecyl chains are molten, the basic lamellar structure still persisted. The slightly larger lamellar thickness of 12.94 nm in the second crystalline state might have been due to an increase in the specific volume of the alkyl peripheries at the melting transition. The structural information was further confirmed by the TEM results. In Figure 4c,d, both images represent alternating layers. The interlayer distances were estimated to be about 12.0 nm, which is in agreement with the SAXS data. As compared with the columnar assemblies of copolymers **1** and **2**, copolymer **3** displayed lamellar assemblies in the solid states, despite having the same dendron ends. The melting transition (39.9 °C) of the longer PEO coil (M_n = 4000 g/mol)

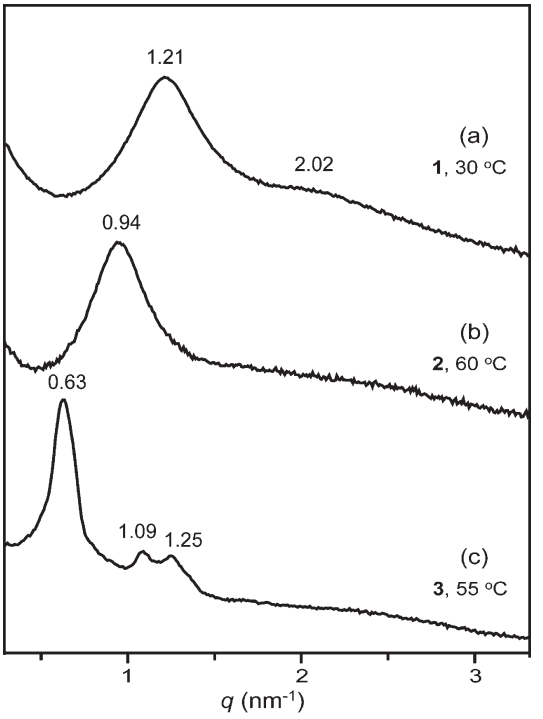

Figure 8. SAXS patterns of copolymers **1**−**3** in the mesophases.

occurred after the melting (25.3 °C) of the tetradecyl peripheries, as demonstrated by the WAXS data. Thus, the driving force for the lamellar organization must be the PEO crystallization, which did not happen in copolymers **1** and **2**. We conjecture that the flat interface of the lamellar assemblies might be located between the PEO crystalline and

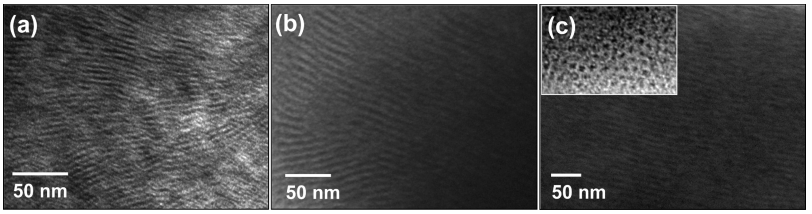

Figure 9. TEM images of ultramicrotomed films at (a) 30 °C for copolymer **1**, (b) 60 °C for copolymer **2**, and (c) 55 °C for copolymer **3** stained with RuO_4. The inset image of (c) at perpendicular beam incidence shows a hexagonal array of PEO cores.

amorphous regions, like a lamellar model proposed by Wang et al.[5f] Consequently, regardless of the morphology of the tetradecyl peripheries, it can be concluded that the lamellar organization is solely dependent upon the crystallization of the PEO coils (Figure 6).

Self-Assembly in the Mesophases (Liquid Crystalline Phases). All triblock copolymers revealed phase-separated microstructures in their mesophases. In order to determine the order−disorder transition temperatures (TODT) at which lattice-disordering transition occurs, the full width at half-maximum (fwhm) of primary peak was plotted versus the reciprocal of temperature in the molten state. In copolymer **1**, fwhm continuously increases as temperature increases, and a typical order−disorder transition is not observed (Figure 7a). This suggests that the molten state of copolymer **1** lacks a lattice ordering. However, the phase is not considered as a conventional liquid state in which blocks are mixed on the molecular level. In Figure 8a, two broad reflections with an approximate q-spacing ratio of 1:1.67 are observed. The broad width of the reflections indicates that the assembled structures lack a long-range order, while the existence of the shoulder-like second reflection suggests that there is still a short-range order. By using the SAXS data only, we could not define the detailed microstructure in the disordered mesophase. Therefore, to characterize it, we carried out TEM experiments at the mesophase temperatures. Figure 9a shows the TEM image of copolymers **1** at 30 °C. The TEM image consists of wavy cylinders, and many structural defects are observed. By taking account of the somewhat disordered packing in the TEM images, the broad reflections in the SAXS data are well elucidated. From the SAXS data, the observed disordered cylindrical structure persisted to 105 °C. Upon further heating to 130 °C, the primary peak was shown to be considerably collapsed, which indicates the loss of the short-range order of the disordered mesophase (data not shown).

Unlike copolymers **1**, copolymers **2** and **3** revealed their order−disorder transitions at 55 and 105 °C in the plots of fwhm vs T^{-1} (Figure 7b,c). In both plots, fwhm shows an abrupt increase at the TODTs. The measured SAXS data below the TODTs showed three reflections with q-spacing ratios of $1:\sqrt{3}:\sqrt{4}$, which is a typical hexagonal columnar pattern (Figures S1 and 8c). The intercylinder distances were estimated to be 8.04 and 11.5 nm for copolymer **2** and **3**, respectively. Consistent with the SAXS results, the TEM images detected at 30 and 55 °C for copolymers **2** and **3** displayed cylindrical arrays (Figures S2a and 9c). As compared with the TEM image of the disordered mesophase of copolymer **1** (Figure 9a), the cylinders in the TEM images of copolymers **2** and **3** were less wavy, and the order of cylinder packing was enhanced. This TEM observation is consistent with the well-resolved SAXS data. As shown in the inset of Figure 9c, RuO_4-stained dark PEO cylindrical cores surrounded by the tetradecyl matrix were observed. Considering the volume fractions (f_v = 0.55 and 0.44) of the tetradecyl peripheries in copolymers **2** and **3**, the observed morphological behavior suggests that the phase boundaries in the triblock copolymer system are significantly shifted toward larger volume fractions of the linear PEO chain when compared with conventional linear block copolymers. This is consistent with theoretical predictions.[15]

Like copolymer **1**, copolymers **2** and **3** exhibited disordered mesophases above the TODTs. As compared to their ordered hexagonal columnar mesophases, the SAXS data showed broader and less intense reflections (Figures 8b and S1b), and the TEM results displayed somewhat irregular cylinders (Figures 9b and S2b). In the SAXS data, the primary peaks persisted to the experimentally accessible temperature of 200 °C, although the intensities decreased as temperature increased. This suggests that the cylinders with a lack of the long-range order exist up to 200 °C.[16] It is interesting to note that the disordered phase in this study consists of cylinders rather than spherical micelles or layers.[17] The driving force for the generation of the disordered cylindrical phase is currently under investigation.

Conclusions

We prepared a series of three triblock copolymers **1**−**3**, which consist of aliphatic polyether third-generation dendrons with tetradecyl peripheries and hydrophilic linear PEOs of different coil lengths. The DSC and WAXS analyses demonstrated that the PEO crystallinities of copolymers **1**−**3** were significantly reduced, and notably the PEOs of copolymers **1** and **2**, they completely lost their crystallinity. This reduction or elimination is attributed to the large cross section of the third-generation dendron preventing the PEOs from having extended conformations as well as by a plasticization effect caused by the PEO-like dendritic core. For the tetradecyl crystallinities, copolymers **1** and **2** revealed similar values of 33% and 34%, while copolymer **3** exhibited a somewhat higher value of 41%. This might be attributed to the hard confinement effect by the crystalline PEO regions during the crystallization of the tetradecyl peripheries. The self-assembling behavior in the solid states was shown to be complicated as a function of PEO coil length. Copolymers **1** and **2**, with the amorphous PEO coils, self-assemble into oblique and rectangular columnar structures, respectively. In contrast, copolymer **3** with a crystalline PEO coil organizes into lamellar structures in both of its crystalline states. In their molten states, all triblock copolymers showed microphase-separated microstructures. As indicated by SAXS and TEM data, copolymer **1** exhibited a disordered cylindrical mesophase, while copolymers **2** and **3** displayed ordered hexagonal columnar and disordered cylindrical mesophases upon heating. Consequently, in the designed dendritic−linear−dendritic block copolymers, complex thermal and bulk assembling behaviors in the solid and molten states can be modulated by a simple variation of the middle PEO length.

Acknowledgment. This work was supported by the Korea Research Foundation (D00128), the Korea Science and Engineering Foundation (R01-2006-000-11221-0), and the GRRC program (67345) of Gyeonggi province. We acknowledge the Pohang Accelerator Laboratory (Beamline 10C1), Korea.

Supporting Information Available: Synthetic and other experimental details. This material is available free of charge via the Internet at http://pubs.acs.org.

References and Notes

(1) (a) Hamley, I. W. *The Physics of Block Copolymers*; Oxford University Press: New York, 1998.(b) Hillmyer, M. A.; Bates, F. S.; Almdal, K.; Mortensen, K.; Ryan, A. J.; Fairclough, J. P. A. Science 1996, 271, 976–978. (c) Floudas, G.; Vazaiou, B.; Schipper, F.; Ulrich, R.; Wiesner, U.; Iatrou, H.; Hadjichristidis, N. Macromolecules 2001, 34, 2947–2957.

(2) (a) Gitsov, I.; Wooley, K. L.; Hawker, C. J.; Ivanova, P. T.; Fréchet, J. M. J. *Macromolecules* **1993**, *26*, 5621–5627. (b) Gitsov, I.; Fréchet, J. M. J. *Macromolecules* **1994**, *27*, 7309–7315. (c) Leduc, M. R.; Hawker, C. J.; Dao, J.; Fréchet, J. M. J. *J. Am. Chem. Soc.* **1996**, *118*, 11111–11118. (d) Zhu, L.; Tong, X.; Li, M.; Wang, E. *J. Polym. Sci., Part A: Polym. Chem.* **2000**, *38*, 4282–4288. (e) Zhao, Y.-L.; Jiang, J.; Liu, H.-W.; Chen, C.-F.; Xi, F. *J. Polym. Sci., Part A: Polym. Chem.* **2001**, *39*, 3960–3966. (f) Mecerreyes, D.; Dubois, P. H.; Jérôme, R.; Hendrick, J. L.; Hawker, C. J. *J. Polym. Sci., Part A: Polym. Chem.* **1999**, *37*, 1923–1930. (g) Connal, L. A.; Vestberg, R.; Hawker, C. J.; Qiao, G. G. *Macromolecules* **2007**, *40*, 7855–7863. (h) Emrick, T.; Hayes, W.; Fréchet, J. M. J. *J. Polym. Sci., Part A: Polym. Chem.* **1999**, *37*, 3748–3755. (i) Al-Muallem, H. A.; Knauss, D. M. *J. Polym. Sci., Part A: Polym. Chem.* **2001**, *39*, 152–161. (j) Froimowicz, P.; Paez, J.; Gandini, A.; Belgacem, N.; Strumia, M. *Macromol. Symp.* **2006**, *245−246*, 51–60.

(3) (a) Vavasour, J. D.; Whitmore, M. D. *Macromolecules* **1993**, *26*, 7070–7075. (b) Milner, S. T. *Macromolecules* **1994**, *27*, 2333–2335.

(4) (a) Chapman, T. M.; Hillyer, G. L.; Mahan, E. J.; Shaffer, K. A. *J. Am. Chem. Soc.* **1994**, *116*, 11195–11196. (b) van Hest, J. C. M.; Delnoye, D. A. P.; Baars, M. W. P. L.; van Genderen, M. H. P.; Meijer, E. W. *Science* **1995**, *268*, 1592–1595. (c) van Hest, J. C. M.; Baars, M. W. P. L.; Elissen-Román, C.; van Genderen, M. H. P.; Meijer, E. W. *Macromolecules* **1995**, *28*, 6689–6691. (d) Iyer, J.; Fleming, K.; Hammond, P. T. *Macromolecules* **1998**, *31*, 8757–8765. (e) Chang, Y.; Kwon, Y. C.; Lee, S. C.; Kim, C. *Macromolecules* **2000**, *33*, 4496–4500. (f) Aoi, K.; Motoda, A.; Okada, M.; Imae, T. *Macromol. Rapid Commun.* **1997**, *18*, 945–952. (g) Barriau, E.; Marcos, A. G.; Kautz, H.; Frey, H. *Macromol. Rapid Commun.* **2005**, *26*, 862–867. (h) Gillies, E. R.; Jonsson, T. B.; Fréchet, J. M. J. *J. Am. Chem. Soc.* **2004**, *126*, 11936–11943. (i) Tian, L.; Hammond, P. T. *Chem. Mater.* **2006**, *18*, 3976–3984.

(5) (a) Percec, V.; Tomazos, D.; Heck, J.; Blackwell, H.; Ungar, G. *J. Chem. Soc., Perkin Trans. 2* **1994**, 31–44. (b) Román, C.; Fischer, H. R.; Meijer, E. W. *Macromolecules* **1999**, *32*, 5525–5531. (c) Mackay, M. E.; Hong, Y.; Jeong, M.; Tande, B. M.; Wagner, N. J.; Hong, S.; Gido, S. P.; Vestberg, R.; Hawker, C. J. *Macromolecules* **2002**, *35*, 8391–8399. (d) Pochan, D. J.; Pakstis, L.; Huang, E.; Hawker, C.; Vestberg, R.; Pople, J. *Macromolecules* **2002**, *35*, 9239–9242. (e) Magbitang, T.; Lee, V. Y.; Cha, J. N.; Wang, H.-L.; Chung, W. R.; Miller, R. D.; Dubois, G.; Volksen, W.; Kim, H.-C.; Hedrick, J. L. *Angew. Chem., Int. Ed.* **2005**, *44*, 7574–7580. (f) Duan, X.; Yuan, F.; Wen, X.; Yang, M.; He, B.; Wang, W. *Macromol. Chem. Phys.* **2004**, *205*, 1410–1417.

(6) (a) Cho, B.-K.; Jain, A.; Gruner, S. M.; Wiesner, U. *Science* **2004**, *305*, 1598–1601. (b) Cho, B.-K.; Jain, A.; Mahajan, S.; Ow, H.; Gruner, S. M.; Wiesner, U. *J. Am. Chem. Soc.* **2004**, *126*, 4070–4071. (c) Johnson, M. A.; Iyer, J.; Hammond, P. T. *Macromolecules* **2004**, *37*, 2490–2501. (d) Gao, Y.; Zhang, X.; Yang, M.; Zhang, X.; Wang, W.; Wegner, G.; Burger, C. *Macromolecules* **2007**, *40*, 2606–2612. (e) Kim, J.-K.; Hong, M.-K.; Ahn, J.-H.; Lee, M. *Angew. Chem., Int. Ed.* **2005**, *44*, 328–332.

(7) Chung, Y.-W.; Lee, J.-K.; Zin, W.-C.; Cho, B.-K. *J. Am. Chem. Soc.* **2008**, *130*, 7139–7147.

(8) Chung, Y.-W.; Lee, B.-I.; Kim, H.-Y.; Wiesner, U.; Cho, B.-K. *J. Polym. Sci., Part A: Polym. Chem.* **2007**, *45*, 4988–4994.

(9) Takahashi, Y.; Tadokoro, H. *Macromolecules* **1973**, *6*, 672–675.

(10) (a) Hillmyer, M. A.; Bates, F. S. *Macromolecules* **1996**, *29*, 6994–7002. (b) Sun, L.; Liu, Y.; Zhu, L.; Hsiao, B. S.; Avila-Orta, C. A. *Polymer* **2004**, *45*, 8181–8193.

(11) Cho, B.-K.; Jain, A.; Nieberle, J.; Mahajan, S.; Wiesner, U. *Macromolecules* **2004**, *37*, 4227–4234.

(12) Trent, J. S.; Scheinbeim, J. I.; Couchman, P. R. *Macromolecules* **1983**, *16*, 589–598.

(13) Balsamo, V.; von Gyldenfeldt, F.; Stadler, R. *Macromolecules* **1999**, *32*, 1226–1232.

(14) (a) Ponomarenko, S. A.; Boiko, N. I.; Shibaev, V. P.; Richardson, R. M.; Whitehouse, I. J.; Rebrov, E. A.; Muzafarov, A. M. *Macromolecules* **2000**, *33*, 5549–5558. (b) Percec, V.; Won, B. C.; Peterca, M.; Heiney, P. A. *J. Am. Chem. Soc.* **2007**, *129*, 11265–11278.

(15) (a) Frischknecht, A.; Fredrickson, G. H. *Macromolecules* **1999**, *32*, 6831–6836. (b) Grason, G. M.; DiDonna, B. A.; Kamien, R. *Phys. Rev. Lett.* **2003**, *91*, 058304.

(16) (a) Lynd, N. A.; Hillmyer, M. A. *Macromolecules* **2007**, *40*, 8050–8055. (b) Wang, X.; Dormidontova, E. E.; Lodge, T. P. *Macromolecules* **2002**, *35*, 9687–9697.

(17) (a) Lee, M.; Lee, D.-W.; Cho, B.-K.; Yoon, J.-Y.; Zin, W.-C. *J. Am. Chem. Soc.* **1998**, *120*, 13258–13259. (b) Sakamoto, N.; Hashimoto, T.; Han, C. D.; Vaidya, N. *Macromolecules* **1997**, *30*, 1621–1632. (c) Olsen, B. D.; Segalman, R. A. *Macromolecules* **2006**, *39*, 7078–7083.